Solar Energy 219 (2021) 65–74

Contents lists available at ScienceDirect

Solar Energy

journal homepage: www.elsevier.com/locate/solener

Pooling the cable: A techno-economic feasibility study of integrating offshore floating photovoltaic solar technology within an offshore wind park

S.Z.M. Golroodbari [a], D.F. Vaartjes [b], J.B.L. Meit [b], A.P. van Hoeken [b], M. Eberveld [c], H. Jonker [c], W.G.J.H.M. van Sark [a,*]

[a] Copernicus Institute, Utrecht University, Princetonlaan 8A, 3584 CB Utrecht, the Netherlands
[b] Oceans of Energy, Valkenburg Airport, Building 396 Wassenaarseweg 75, 2223 LA Katwijk, the Netherlands
[c] Rijkswaterstaat, Postbus 2232, 3500 GE Utrecht, the Netherlands

ARTICLE INFO

Keywords:
Offshore photovoltaics
Feasibility study
Cable pooling
Economic analysis
Offshore wind

ABSTRACT

In this paper, a techno-economic analysis is performed to assess the feasibility of adding an offshore floating solar farm to an existing Dutch offshore wind farm in the North Sea, under the constraint of a certain fixed cable capacity. The specific capacity of the cable that connects the offshore park to the onshore grid is not fully used due to the limited capacity factor of the wind farm. The principle of cable pooling allows to add floating solar capacity. Using weather data it is found that adding solar capacity leads to forced curtailment due to the cable capacity, but this is quite limited as result of the anti-correlation of the solar and wind resource. For the economic analysis, different scenarios regarding subsidy measures are considered for the calculation of net present value and levelized cost of electricity. Also the optimum additional PV capacity for each scenario is computed. The results show that with higher cost per Wp, optimum PV capacity decreases, but more favourable subsidies lead to higher optimized PV capacities. As the aim of the paper is not limited to a case study a methodology is developed for generalization of the techno-economic analysis of a hybrid solar/wind park. In this generalization, the initial investment, system degradation, cable capacity, number of hours when each system is active, and energy price, are implemented to compute the optimum PV capacity regarding the net present value as an indicator for economic analysis of the project.

1. Introduction

Reaching greenhouse gas emission reduction goals requires massive deployment of renewable energy harvesting technologies such as solar and wind. Energy systems based on renewables are not only feasible, but already economically viable and decreasing in cost every year (Brown et al., 2018; Ram et al., 2017). Besides their intermittent character that poses a challenge for grid integration, another main issue of their increased share is their effect on land scarcity, especially in or close to densely populated areas such as the Netherlands (Gielen et al., 2019; van Zalk and Behrens, 2018; Jäger-Waldau, 2020). Renewables generally require more land than fossil-fuel based electricity power plants, when excluding land use for mining. Hence, larger areas are needed to maintain similar or increased amounts of global electricity demand. Deployment of large wind parks and solar fields has been increasing, but also has met with increased public resistance. This has not only led to the development of offshore wind parks and increased interest in offshore floating solar systems, but also more attention is paid to measures to integrate solar fields in the existing landscape. Here multiple land use is key, while also biodiversity issues and agricultural aspects are being taken into account in their development (Jäger-Waldau, 2020; Scognamiglio and Garde, 2016; Randle-Boggis et al., 2020). Also, it has prompted the Dutch government to explicitly state that deployment of photovoltaic (PV) solar systems should predominantly be done at roofs (Rijksoverheid, 2019), while the huge potential of offshore PV has been recognized in a roadmap for PV systems and applications (Folkers et al., 2017).

In the Netherlands, currently, four offshore wind farms are in

* Corresponding author.
E-mail addresses: S.Z.mirbagherigolroodbari@uu.nl (S.Z.M. Golroodbari), johnny.meit@oceansofenergy.blue (J.B.L. Meit), allard.vanhoeken@oceansofenergy.blue (A.P. van Hoeken), mattijs.erberveld@rws.nl (M. Eberveld), rik.jonker@rws.nl (H. Jonker), W.G.J.H.M.vanSark@uu.nl (W.G.J.H.M. van Sark).

https://doi.org/10.1016/j.solener.2020.12.062
Received 30 June 2020; Received in revised form 23 December 2020; Accepted 24 December 2020
Available online 8 March 2021

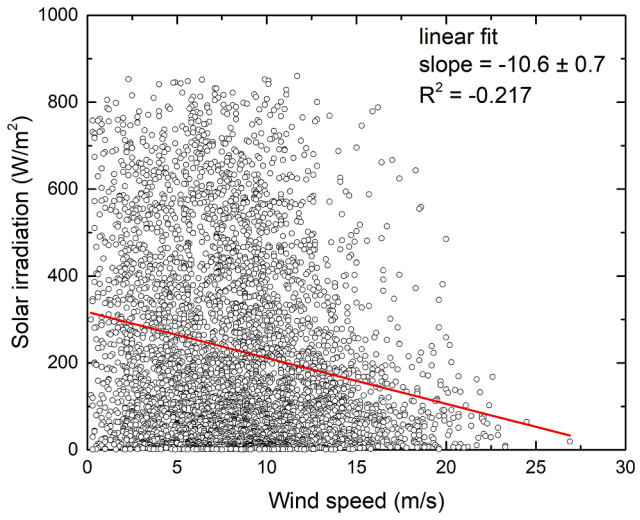

Fig. 1. Solar irradiance and wind speed correlation. Hourly data for 2005.

operation with a total combined capacity of 957 MW. An additional 3450 MW is planned to be developed by 2023 (RVO, 2019). An even faster growth is seen for solar PV. At the end of 2019, nearly 7 GWp was installed (Dutch New Energy Research, 2020), which made for a 5.4% contribution to the national electricity supply. For the realization of the national emission reduction goals for the Netherlands of 49% by 2030 and 95% by 2050 the installed renewables base should be increased substantially. A combination of 20 GW offshore wind, 11 GW on-shore wind, and 29 GW PVp would generate the projected electricity demand of 120 TWh in 2030. For 2050 this should be about doubled. Such large capacities require large areas of roof and façade surfaces and land for PV (Folkers et al., 2017). Due to land availability issues, floating PV has been suggested recently, and several floating PV systems are in operation globally (Rosa-Clot and Tina, 2017). These originally have been based on similar designs as used for land-based systems, as the water bodies on which these are deployed are relatively quiet in terms of wind and waves (Farfan and Breyer, 2018; Sahu et al., 2016). The next more or less logical step is to take PV offshore. As wave and other weather conditions are much more severe at sea, different approaches are needed for large-scale floating PV systems. Much research in this field is being performed at the moment. One aspect is already found to be beneficial for performance, which is the cooling effect of (sea) water leading to higher energy yields (Cazzaniga et al., 2018; Zahra Golroodbari and van Sark, 2020). Beside the technical aspects, the capital- and operational expenditures will also play a role in future development. The floating panels are expected to be more costly than conventional PV panels, due to more corrosion resistant panel designs and extra floating and/or mooring components. Also, installation costs of the panels are expected to be higher. The construction of an offshore grid connection to transport the produced energy to the mainland is another important factor that is expected to increase the total costs per kWh.

Nevertheless, the Netherlands as many other countries surrounded with large bodies of water are considering offshore floating PV as a serious option for renewable energy supply. As an example, the recent Dutch national roadmap on PV potential states an overall potential of 200 + GWp of which most is in the built environment and on land, while it also defines an inland floating PV potential of 24 GWp, and an offshore potential of 45 GWp (Folkers et al., 2017).

Given the large space available in between turbines of a large scale offshore wind park, as well as the already present or planned cable capacity to connect a wind park to the grid on shore, adding floating PV within such an offshore wind park may be a feasible option. The cable has been designed to transport the maximum possible amount of power generated by the wind park, i.e., the rated wind park capacity, while capacity factors may be between 35% and 50% (Arrambide et al., 2019). As shown in Fig. 1, a scatter plot of solar irradiance versus wind speed reveals that they are correlated negatively, albeit weak. Thus, adding solar can be expected to increase the cable capacity factor thus more effectively using the cable (also known as cable pooling), while providing less variable power, in a similar way as coupling wind farms and wave energy generators (Venkataraman et al., 2018; Astariz and Iglesias, 2016). In addition, costs for maintenance, operations and construction could be shared by integrating solar energy within offshore wind farms, leading to overall decreased capital and operational expenditures.

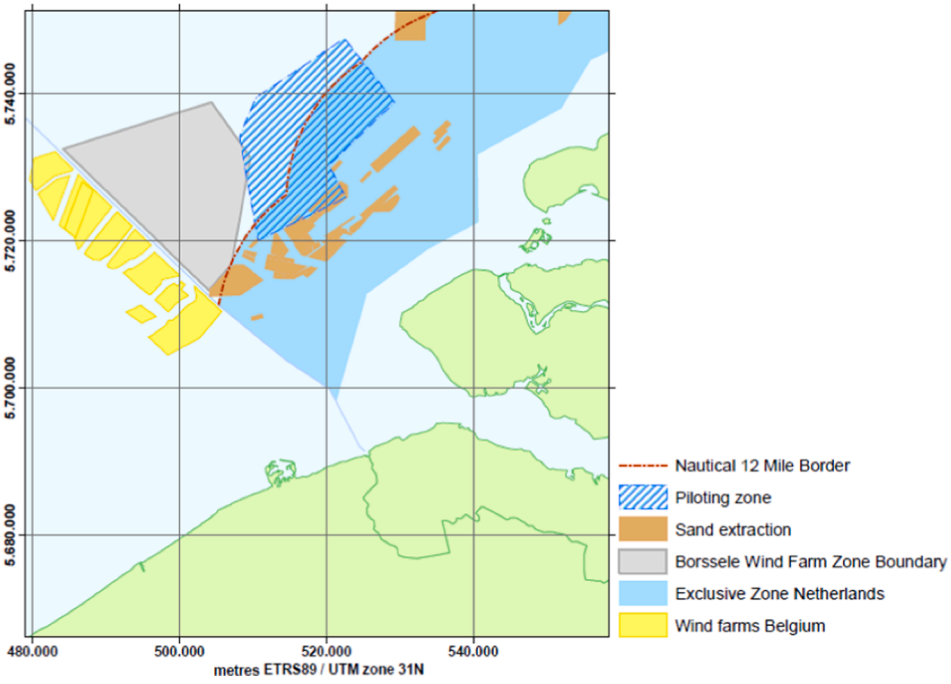

Fig. 2. The Borssele Wind Farm Zone and surrounding areas. Source: RVO RVO (2019).

We do note that the actual area that an offshore PV park would need to generate 1 GWh is about 2–11 times smaller than required for an offshore wind park. Due to inter-turbine distances of at least 5 times the rotor diameter to limit wake effects, the power density of a wind park ranges from 5–10 MW/km^2, while it is about 100–200 MWp/km^2 for a solar PV park. Nevertheless, capacity factor differences lead to a energy density of about 15–44 GWh/km^2 for a wind park versus about 90–180 GWh/km^2 for a solar park in the Netherlands, with 35–50% capacity factor for wind (Arrambide et al., 2019) and 10% capacity factor for PV (Van Sark et al., 2014). Hence, this difference in area usage would leave sufficient room for any maintenance ships required to sail through the wind park, and at the same time would lead to minimal ecological disturbances due to shading of the sea subsurface (Karpouzoglou et al., 2020).

In this paper we will perform a techno-economic feasibility study of incorporating an offshore floating PV system in a planned wind park of 752 MW rated capacity in the North Sea, with a planned transport cable capacity of 700 MW. We note here that as the power production by the wind farm is mostly lower than the rated capacity, the cable capacity is not used fully. Even at rated capacity, wake losses lead to sub-optimal usage of cable capacity. A decrease of efficiency and increase of downtime of the wind farm over its lifetime will result in a further sub-optimal usage of cable capacity, hence a solar park can make use of leftover cable capacity. In Section 2, we will describe the hybrid wind solar park and present the methodology used to determine energy generation by PV and wind turbines, and how to find an optimum configuration in terms of economics. In Section 3 results are presented and discussed. It also provides suggestions on how to generalize the results obtained, given site-specific meteorological conditions, and technical and economical aspects. Section 4 provides a conclusion and outlook for further research.

2. Method

In this section details of the case study wind farm Borssele are described, followed by a description of combining it with a possible floating PV system. Also, different scenarios for an economical analysis will be reviewed.

2.1. Wind park site description

We focus our analysis on a planned wind park, denoted as Borssele wind park I & II, based on the report published by the Dutch Enterprise Agency RVO (RVO, 2019). This report contains a detailed description of the Borssele Wind Farm Zone (BWFZ), a collection of data regarding the physical environment of the Borssele sea area, detailed information on national subsidy grant related issues and a legal framework for application of this grant. The BWFZ is located at the southern border of the Netherlands Exclusive Economic Zone (EEZ) at 51.583° N, 3°E, approximately 500 m from the Belgium border, see Fig. 2. The first Siemens Gamesa 8 MW turbines with rotor diameter of 167 m have been installed recently by wind park developer Ørsted, and the park should be fully operational by the end of 2020 (Orsted).

The BWFZ has an area of approximately 234 km^2, but it covers 344 km^2 with maintenance and safety zones included. The BWFZ is surrounded by a sand extraction area, piloting zone, shipping lanes and anchoring locations as well as Belgium wind farms, just south-west of the zone. Total planned rated capacity of those parks is about 600 MW of which about 230 MW is operational already.

Although existing infrastructure such as pipelines and telecommunication cables cross the BWFZ, cost of relocating these was too high, and as a consequence planning of the wind turbine construction is taking the existing infrastructure into account. On both sides of the Dutch-Belgian border a safety zone of 500 m is defined. The same safety zone of 500 m is applied to both sides of the cables and pipelines that run through the BWFZ. Between Borssele I & II, a shipping corridor is in place, going from east to west. The national transmission system operator (TSO) TenneT has planned to install two offshore substations: Borssele Alpha and Borssele Beta (Tennet, 2019). The substation Alpha will connect Borssele I & II to the onshore electricity grid via a 700 MW capacity cable.

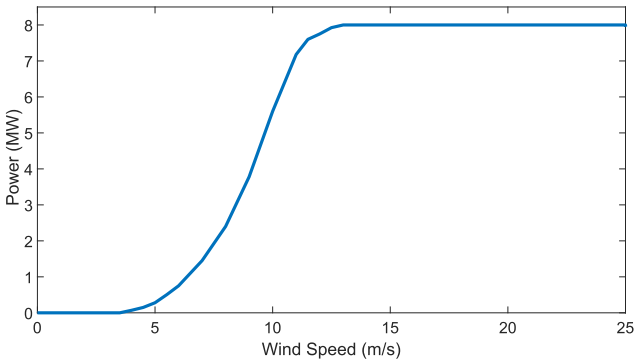

Fig. 3. Power curve of the Gamesa 8 MW wind turbine (Siemens, 2021).

2.2. System modeling

In order to study the feasibility of the hybrid power system, which is described before, we need to use a precise mathematical model. With that model we will be able to perform a technical and economic analysis.

The goal of the technical analysis is to estimate the total energy production of the combined wind solar farm. The analysis is divided into three main steps:

1. based on historical wind data, the potential energy production of the Borssele I & II wind farm will be calculated;
2. based on historical solar irradiance data, the potential energy production of a floating PV system will be calculated for different PV system sizes;
3. these two data sets are then combined to estimate the total energy production of the complete system.

We use an hourly time resolution throughout this paper. The cable capacity of 700 MW limits the energy transmission from the offshore system to the mainland, so optimizing annual energy production should be performed using the 700 MW cable constraint.

In the following subsections we will first describe the wind park and the solar park model individually, which is based on a wind turbine model as well as a solar module model. The next step is the methodology for calculating the annual energy as well as energy per hour. After that, an economic analysis will be described, using different scenarios for subsidy schemes.

2.3. Offshore wind model

The modeling of the offshore wind park has two main steps: (i) calculating the optimal potential power output of wind turbines, and (ii) implementing the limitations of the wind park in which the turbines are part of. The offshore wind farm will consist of 94 Siemens Gamesa wind turbines of 8 MW capacity each. Fig. 3 shows the power curve of such a turbine. The extracted specifications of the wind turbine from the power curve are cut-in speed of 3.5 m/s, cut-out speed of 25 m/s, and rated power wind speed of 13 m/s. To calculate the generated amount of power at a certain moment it is required to multiply the hourly wind speed data by the power curve.

2.3.1. Wind farm performance

The conversion of wind energy to useful electrical energy involves two processes: (i) the primary process of extracting kinetic energy from

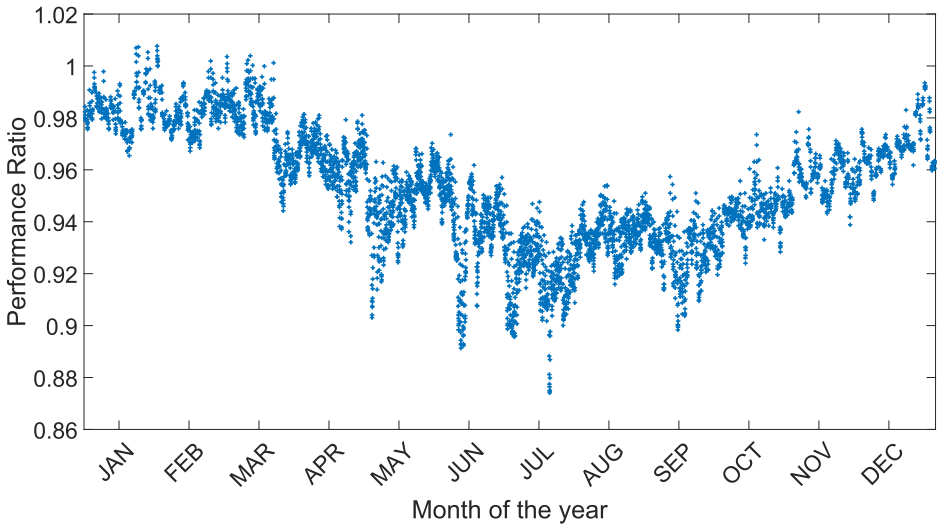

Fig. 4. PV module DC *PR* for the year 2006, illustrating the effect of temperature.

wind and conversion to mechanical energy at the rotor axis, and (ii) the process of the conversion into useful energy, mostly electrical (Vermeer et al., 2003). One of the important issues in the first process is the wind turbine wake effect decreasing the total conversion efficiency of a wind park. Bulder et al. (2014) have studied the wake effect and wind farm power density and they concluded that in general the higher the power density of a wind park, the lower the efficiency due to the larger wake effects. Wind farm efficiency of the Borssele location has been estimated in Bulder et al. (2014) considering a turbine capacity of either 6 MW or 8 MW, and by wind farm power density, 6 and 9 MW/km^2. The wind farm design that is the most applicable for this research is expected to achieve an efficiency of 91.4% on annual basis, hence a 8.6% loss compared to combining single wind turbines. Wake effects are accounted for by adjusting wind velocities based on the model by Jensen (1983), Katic et al. (1987). This leads to a park efficiency of 90%.

The hourly ($E_{WF,h}$) and annual ($E_{WF,a}$) wind farm energy production is shown in Eqs. (1) and (2).

$$E_{WF}(h) = N_{WT}\ E_{WT}(h) \tag{1}$$

$$E_{WF,a} = \sum_{h} E_{WF}(h) \tag{2}$$

in which N_{WT} is the number of wind turbines in the farm, which is 94 in this case, and $E_{WT}(h)$ is the hourly (h) generated energy per wind turbine with respect to wind speed.

All machinery experiences an unrecoverable loss in performance over time. The energy produced by a wind farm gradually decreases over its lifetime, due to falling availability, aerodynamic performance or conversion efficiency (Staffell and Green, 2014). If capacity factors decrease significantly with age, wind farms will produce a lower cumulative lifetime output, increasing the levelized cost of electricity (LCOE) of the wind farm. Based on the research presented in Staffell and Green (2014) it is assumed that the level of degradation of the Borselle I & II wind farm's output is 12% over a twenty year lifetime (0.6% per year). Therefore, the Borssele wind farm energy production over time is calculated as shown in Eq. 3.

$$E_{WF,N_{year}} = \sum_{n=1}^{N_{year}} E_{WF,1} \times (1 - 0.006)^{n-1} \tag{3}$$

where $E_{WF,N_{year}}$ is the cumulative amount of energy generated by the wind farm, $E_{WF,1}$ the energy generated by the wind farm in the first year, n is the summation index and N_{year} is the total number of years the whole system is considered to be operational.

2.4. Solar farm performance

The modeling of the power output of the floating solar PV system is built on the same reasoning as with the offshore wind farm. First the optimal performance of the floating solar PV system was calculated, after which limitations were applied. Eqs. (4) and (5) are used to compute the annual generated energy from one solar panel in the solar farm.

$$E_{PV}(h) = PR\ \eta_{PV} A_{PV} G(h) \tag{4}$$

$$E_{PV,a} = \sum_{h} E_{PV}(h) \tag{5}$$

where $E_{PV}(h)$ is hourly generated energy of one PV module (kWh), $E_{PV,a}$ is annual generated energy (kWh), $G(h)$ is solar irradiation per hour (Wh/m^2), A_{PV} is panel area (m^2), η_{PV} is panel efficiency, and PR is the performance ratio to account for system loss (Reich et al., 2012).

In this research, it is assumed that the solar panel is a 1.6 m^2 crystalline silicon panel which has rated maximum power point P_{MPP} of 300 Wp (hence $\eta_{PV} = 18.8\%$). The efficiency is a function of temperature (T), the temperature coefficient of power used here is -0.375%/K, which is extracted from the specification sheet of an Exasun X60-BG300 module (Exasun, 2018). Temperature and other system losses including DC-AC conversion by inverters used are all accounted for in the performance ratio PR (Reich et al., 2012). As an example, for the irradiation and temperature data for the year 2006 at the wind park location, Fig. 4 shows DC performance ratio (PR), illustrating the effect of temperature, i.e., performance ratio is lower in summer than in winter (Nordmann et al., 2015). In addition, the strong dips observed in summer are due to high ambient temperatures that occurred for short periods of time.

Eqs. (4) and (5) calculate the annual energy output of a single panel. In order to calculate the total energy output of the solar farm of a certain capacity, this result should be multiplied with the total number of solar panels N_{PV} corresponding with the installed solar capacity. For example, a 1 MWp system contains 3333 panels, which would require an area of 0.0053 km^2, following a horizontal design. Hourly and annual PV farm outputs thus are:

$$E_{PVF}(h) = N_{PV} E_{PV}(h) \tag{6}$$

$$E_{PVF,a} = N_{PV} E_{PV,a} \tag{7}$$

Except for the rotating blades of the wind turbines, shading effects on solar panels that would reduce solar park efficiency can be ignored. However, there is a decay of the efficiency of a solar panel over its

lifetime. An accurate quantification of power decline over time, also known as degradation rate, is essential to all stakeholders, utility companies and researchers alike. A statistical approach based on historical data has been reported to quantify degradation rates (Jordan and Kurtz, 2012): the efficiency of solar panels reduces with 0.5 percent per year on average. The total energy production of the solar farm over its lifetime thus can be calculated in Eq. (8):

$$E_{PV,N_{year}} = \sum_{n=1}^{N_{year}} E_{PV,1} \times (1 - 0.005)^{n-1} \tag{8}$$

where $E_{PV,N_{year}}$ is the cumulative energy output of the solar panel over its lifetime, and $E_{PV,1}$ is the energy output of the solar panel in the first year. As above, the total energy output of the solar farm is calculated by multiplying with the number of panels, as in Eq. (7).

2.5. Capacity factor

The capacity factor is calculated using the following equation. It is equivalent to the amount of full load hours in a year.

$$CF = \frac{\text{actual output (MWh)}}{\text{nominal power (MW)} \times 365 \times 24} \times 100\ (\%) \tag{9}$$

2.6. Optimizing the combined wind solar system

The main constraint in this research is that the power transmission cable has a maximum capacity of 700 MW which limits the total amount of power that can be produced by the floating solar panels and the wind park without congesting the power transmission cable. In this research, it is assumed that if the combined solar and wind power production is over 700 MW, the solar output will be curtailed to a value which can vary between 0–100%, meaning that they will not deliver full power to the grid at that time. Note that we have conveniently chosen an hourly time resolution. The power constraint of 700 MW thus translates to an energy constraint of 700 MWh. The total energy production of the combined energy system is therefore calculated as follows, with C_{PV} the curtailment ratio (0–100%):

$$E_{tot}(h) = E_{WF}(h) + C_{PV}E_{PVF}(h) \leqslant 700 \text{ for } h \in [1, 8760] \tag{10}$$

The optimization problem here is defined as

$$\min\{\texttt{costofelectricity}\},\ \textbf{subject to}\ \{\texttt{cableconstraints}\} \tag{11}$$

2.7. Economic analysis

The outcomes of the technical analysis give insight on the amount of energy that can be generated by integrating solar panels in offshore wind farms. The goal of the economic analysis is to evaluate the economic value of the produced energy and to provide insight on how much such an energy system may cost. Therefore, the first step of the economic analysis was to determine the value of the produced energy.

2.7.1. Determination of the value of energy

In order to calculate the value of generated electricity by the complete system, we consider the (i) market price, (ii) cost of grid connection, and (iii) value of renewable energy. The aforementioned issues will be studied in the following.

2.7.2. Market price

Since the energy market system is complex and many factors influence the energy price, which in addition can fluctuate considerably, we took average annual energy prices based on the Amsterdam Power Exchange (APX) market, now part of European Power Exchange (EPEX). The APX market distinguishes energy prices in a peak (8am - 8 pm) and off-peak price (8 pm - 8am). Table 1 shows the yearly APX price between 2010 and 2018. Average values are 52.9±7.8 €/MWh and 39.9±6.4 €/MWh for peak and off-peak prices, respectively. As there is a large uncertainty in predicting future energy prices, for simplicity the rounded average values of 50 €/MWh and 40 €/MWh for peak and off-peak prices are assumed, respectively. From now on in this paper, the market price is denoted as $\pi_{APX,i}$ with subscript i being p or op for peak and off-peak price, respectively.

Table 1
Yearly average APX Price.

Year	$\pi_{APX,p}$ (€/MWh)	$\pi_{APX,op}$ (€/MWh)
2010	56.01	39.41
2011	61.59	46.81
2012	58.18	42.45
2013	61.16	46.87
2014	48.36	37.22
2015	47.16	36.16
2016	39.30	28.32
2017	46.27	35.50
2018	57.97	46.77
Average	52.89	39.94

2.7.3. Cost of grid connection

The cost of the grid connection of offshore wind farms is considered as social cost, meaning that the government is willing to pay this cost to facilitate the generation of offshore energy. This is also the case with the Borssele wind farm grid connection. The total grid connection cost of the Borssele location is $\pi_{og} = 0.015$ €/kWh (Beurskens and Lensink, 2017).

2.7.4. Value of renewable energy

Despite the availability of several subsidy schemes to stimulate the development of renewable energy technologies in the Netherlands, there are no subsidies specifically designed for offshore floating solar systems yet. Since it is unclear what subsidies will be granted for this type of technology in the future, there are three scenarios developed with each a different level of subsidy.

2.7.4.1. Scenario one: No subsidies for offshore floating solar technologies. In this scenario the total energy value $\pi_{no,i}$ is calculated as follows:

$$\pi_{no,i} = \pi_{APX,i} + \pi_{og},\ i \in [p, op] \tag{12}$$

2.7.4.2. Scenario two: Stimulation of Sustainable Energy Production (SDE+). Energy producers can receive financial compensation for the renewable energy they generate. It is not always profitable to produce renewable energy as the generation cost is higher than the market price. This price difference is the unprofitable part. The subsidy scheme SDE + compensates the unprofitable component for some years, i.e. 15 years. The compensation depends on the renewable energy technology used. The SDE + subsidy is an operating grant. The price for the production of renewable energy is capped (base sum). For the Borssele Wind Farm Location the base sum is set at $\pi_{SDE+} = €125$/MWh (Ministry of Economic Affairs and Climate, 2020). Thus, the total energy value $\pi_{BS,i}$ is calculated as follows:

$$\pi_{BS,i} = \pi_{SDE+} - \pi_{APX,i},\ i \in [p, op] \tag{13}$$

and the total price scenario 2 is

$$\pi_{SDE,i} = \pi_{APX,i} + \pi_{BS,i} + \pi_{og},\ i \in [p, op] \tag{14}$$

2.7.4.3. Scenario three: maximum subsidy (doubled SDE+). It is assumed that because the floating solar technology is still in its development phase, the government is willing to grant the double amount of money per MWh compared with the amount that was reserved for the Borssele

Table 2
Different scenarios subsidy and price comparison.

Scenario	Subsidy (€/MWh)		Price (€/MWh)	
	Peak	Off-Peak	Peak	Off-Peak
1: no subsidy	0	0	65	55
2: SDE+	75	85	140	140
3: doubled SDE+	200	210	265	265

II location (scenario 2). For that reason scenario 3 assumes a cap of the subsidy of $\pi_{SDE+,max} = 250\ €/\text{MWh}$ (doubled SDE+) and the total energy value is calculated as follows:

$$\pi_{max,i} = \pi_{SDE+,max} - \pi_{APX,i},\ \ i \in [p, op] \tag{15}$$

and the total price scenario 3 (doubled SDE+) is

$$\pi_{2SDE,i} = \pi_{APX,i} + \pi_{max,i} + \pi_{og},\ \ i \in [p, op] \tag{16}$$

Prices for all mentioned scenarios per peak and off-peak are summarized in Table 2.

2.8. Lifetime benefits

With the total value for the generated energy determined in the previous steps, the last step is the calculation of the total revenue of the combined wind and floating solar PV system over its lifetime. First the total revenue Π_a for each year was calculated by the following equation:

$$\Pi_a = \sum_h \left(E_p(h)\pi_p + E_{op}(h)\pi_{op}\right) \tag{17}$$

where $E_i(h)$ is hourly energy production (MWh), π_i is price of energy in $€/\text{MWh}$, and $i \in [p, op]$.

Assuming a interest rate of 3%, the net present value *NPV* of the benefits over the energy system's lifetime are then calculated with the following equation:

$$NPV = F_0 + \sum_{n=1}^{N_{year}} \frac{F_n}{(1+r)^n} \tag{18}$$

where F_n is cash-flow after n years, r is interest rate, n is summation index, and N_{year} it the total number of years. The inclusion of the F_0 term is important in the above formula. A typical investment project involves a large negative F_0 which is the initial investment, with positive future cash flows, a combination of revenues and the expenses which are expecting to return the initial investment. For this study we consider F_n as:

$$F_n = \Pi_{a,n} - Opex_n \tag{19}$$

where *Opex* is expenditures for operation and maintenance and is assumed to be 2% of the initial investment which is higher that what is mentioned in Jäger-Waldau (2019) which is 1.35%. Therefore, Eq. (20) is derived as follows:

$$NPV = \sum_{n=1}^{N_{year}} \frac{\Pi_{a,n}}{(1+r)^n} - F_0 \times (1 + 0.02 \times N_{year}) \tag{20}$$

Thus, NPV is an indicator of how much value an investment or project adds to the firm.

Another metric of interest is Levelized Cost of Electricity or (LCOE), which can be defined as the NPV divided by the amount of generated energy E_{tot} during a system's lifetime, which is N_{year}:

$$LCOE = \frac{NPV}{E_{tot}} \tag{21}$$

where E_{tot} is the sum of total wind and solar energy, as given in Eqs. (3) and (8).

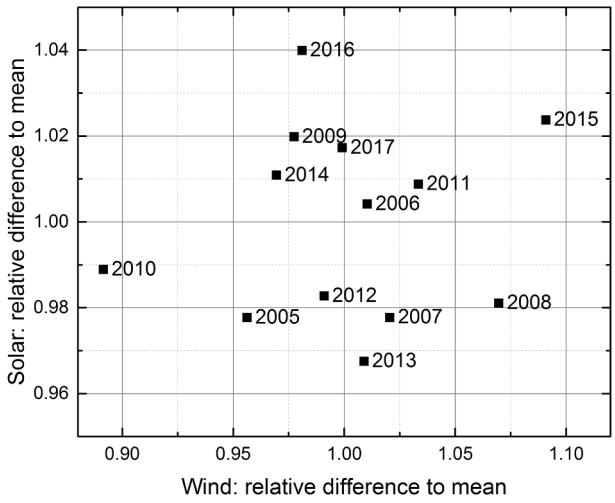

Fig. 5. Scatterplot of solar and wind resource compared to the mean of each resource. Annual solar irradiance (kWh/m^2/yr) and average annual wind speed (m/s) have been used.

3. Results and discussion

The results of the techno-economical analysis are divided into two main parts: (i) the technical analysis results and (ii) the economic analysis results. The technical analysis section provides information on the production potential of floating solar energy within the offshore wind farms. The economic analysis shows what the potential financial benefits are of integrating offshore solar and wind on the North Sea.

3.1. Meteorological data

The wind data used in this research was extracted from the KNMI North Sea Wind (KNSW) atlas (Wijnant et al., 2019), for the years 2005–2017. It provides validated data on a horizontal grid of 2.5 km spatial resolution. Within the Borssele wind farm area a total of 18 data points were used to calculate the average hourly wind speed of the whole area for each year separately, at the hub height of the turbine.

The solar data was extracted from the Copernicus Atmosphere Monitoring Service (CAMS) Radiation Service database (Copernicus Atmosphere Monitoring, 2021). This database provides hourly solar radiation data for the period of 2005–2017, expressed in Wh/m^2. Data was extracted for the latitude and longitude of the solar farm.

3.2. Technical results

The main goal of the technical analysis is to provide reliable energy production data that can be used for the economic analysis. The first step was therefore to determine a base year that can be used to estimate the energy production potential over the system's lifetime.

3.2.1. Base year

For assigning the base year the average total production per year is compared considering data between years 2005 and 2017. Fig. 5 shows that year 2006 is the best option as the solar and wind data both are the closest to the average values. We did not use a typical meteorological year as the correlation between wind and solar would be lost. We note that interannual variations in wind speed are large than solar irradiance variations.

3.2.2. Energy generation

Fig. 6 shows scatter plots of the hourly energy generation of the

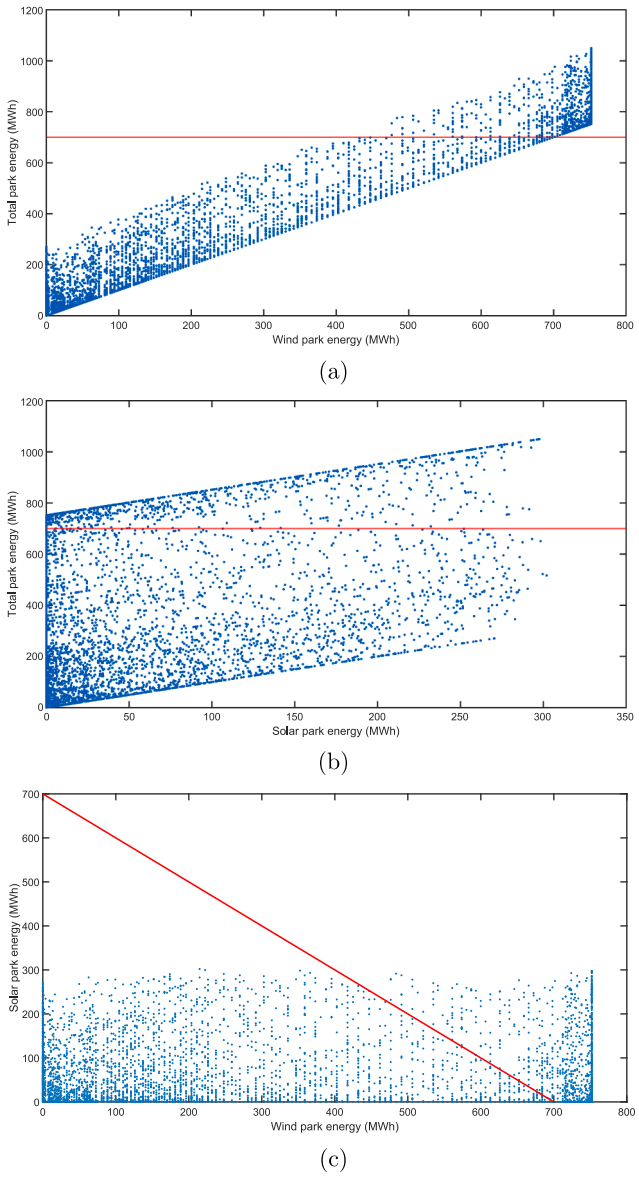

Fig. 6. Scatter plots for a combined solar and wind park of 300 MWp and 752 MW capacity, respectively, for the year 2006. For some hours the cable constraint of 700 MW (red line) is surpassed. (a) total park energy versus wind power, (b) total park energy versus solar power, (c) solar versus wind park energy. (For interpretation of the references to colour in this figure legend, the reader is referred to the web version of this article.)

combined wind and solar park of capacity 752 MW and 300 MWp, respectively, for the year 2006, using the methods outlined in Section 2. It can be seen that by adding solar capacity, more energy can be transported via the cable which thus is more effectively used. However, for some hours in the year the cable capacity of 700 MW is exceeded. Increasing the solar capacity from 300 MW upwards will lead to violations of maximum cable capacity to occur more often. For this particular year, we calculate a capacity factor of 46.49% and 14.05%, respectively. Table 3 shows the effect on adding multiples of 100 MWp solar capacity to the 752 MW wind park. For example, although the number of hours per year that cable capacity is exceeded is increasing to 12.07% for 300 MWp of added solar capacity, curtailed energy is only 1.72%.

For the base year 2006, we find that for $G(h) \neq 0$ there were 4480 hours with non-zero wind speed. We find that for 83% of that amount of hours, the wind farm does not operate optimally (at full capacity), so the full cable capacity is not used thus allowing to add solar power. Full

Table 3
Effect of adding multiples of 100 MWp PV capacity to the 752 MW wind park. The number of hours that cable limit is exceeded increases, as well as curtailed energy.

PV capacity (MWp)	number of hours >700 MWh	generated energy (GWh)	curtailed PV energy (GWh)	relative PV curtailment (%)
0	533	3063	0.0	0.00
100	1036	3186	18.0	0.56
200	1074	3309	37.9	1.14
300	1109	3433	58.9	1.72
400	1165	3556	82.0	2.31
500	1222	3679	107.3	2.92
600	1303	3803	136.6	3.59
700	1432	3927	172.5	4.39
800	1615	4050	219.0	5.41
900	1800	4174	279.1	6.68
1000	1956	4297	349.3	8.13

capacity (at rated power) occurs for 12% of that amount of hours, while no power is generated for 10% or these hours, as the wind speed is lower than the cut-off wind speed (3.5 m/s). For the remaining 78% of hours power is lower than rated power. This is based on the power curve characteristics of the wind turbine (Fig. 3), i.e. full power production for wind speeds in the range of 13 to 25 m/s, and lower power or zero power production for wind speeds between 3.5 and 13 m/s, and 0 and 3.5 m/s, respectively. While the wind park efficiency is not 100% due to wake effects, hourly maximum produced power can be larger than the cabling power limit of 700 MW. This occurs for 533 hours of the year leading to 41 GWh curtailed wind energy, or 1.3%.

3.2.3. Energy production over two decades

It is computed that the Borssele wind farm generates about 60,000 GWh over a period of 20 years. On average, the cable capacity factor is 49.94% without solar panels installed and increases linearly up to 88% with an installed solar capacity of 1.9 GWp. A cable capacity factor of 100% can be obtained for a solar capacity of 2.6 GWp. However, it should be noted that cable capacity is not our only constraint and we need to consider the economical analysis as well.

3.3. Economic analysis

The technical analysis shows that: (i) there is a large potential for floating PV panels within the Borssele I & II wind farm, (ii) there is a limitation on the extra energy that can be produced by adding more solar panels, and (iii) the marginal production potential decreases rapidly with increased installed solar capacity. However, it is necessary to estimate the economical benefits of this combination which we will discuss in this section. Fig. 7 shows the net present value for different scenarios. The initial investment for each Wp for a land based system is assumed 0.6€/Wp (Jäger-Waldau, 2019). To have a better perspective for economic analysis we considered different variations for the initial investment for a floating system as

$$f_{0,FPV} = f_{0,LB} + \gamma,\ \gamma \in [0, 1.25] \tag{22}$$

where γ is an additional price value and $f_{0,FPV}$ and $f_{0,LB}$ are the initial investment for floating and land-based PV system per W_p, respectively. The upper limit is based on recent data reported in Rosa-Clot and Tina (2020). Fig. 7 shows that the relation between *NPV* and PV capacity is not linear and related to the decrease of the marginal power production per extra installed MWp. This figure shows that a very slight change in initial investment for the first scenario (no subsidies) makes the $NPV < 0$. In the optimization problem for this study we should consider both *NPV* and the curtailment energy and solve the problem. Fig. 8 shows the optimum PV capacity for different scenarios with different initial investments over the bar charts which is derived from Fig. 7.

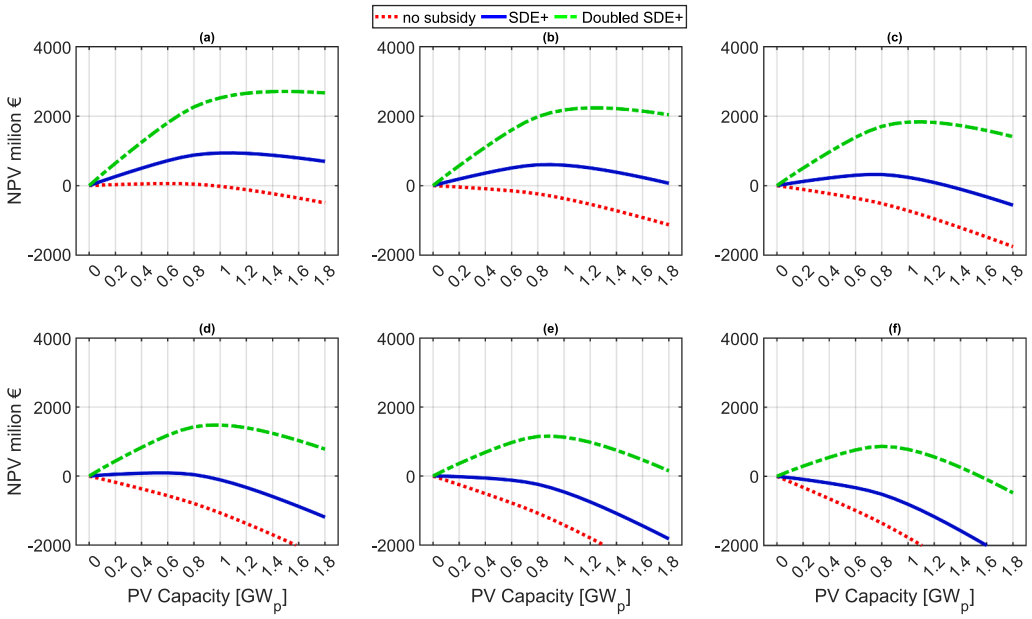

Fig. 7. *NPV* for different scenarios considering the initial investment:. (a) 0.6, (b) 0.85, (c) 1.1, (d) 1.35 , (e) 1.6, (f) 1.85 [$€/W_p$]

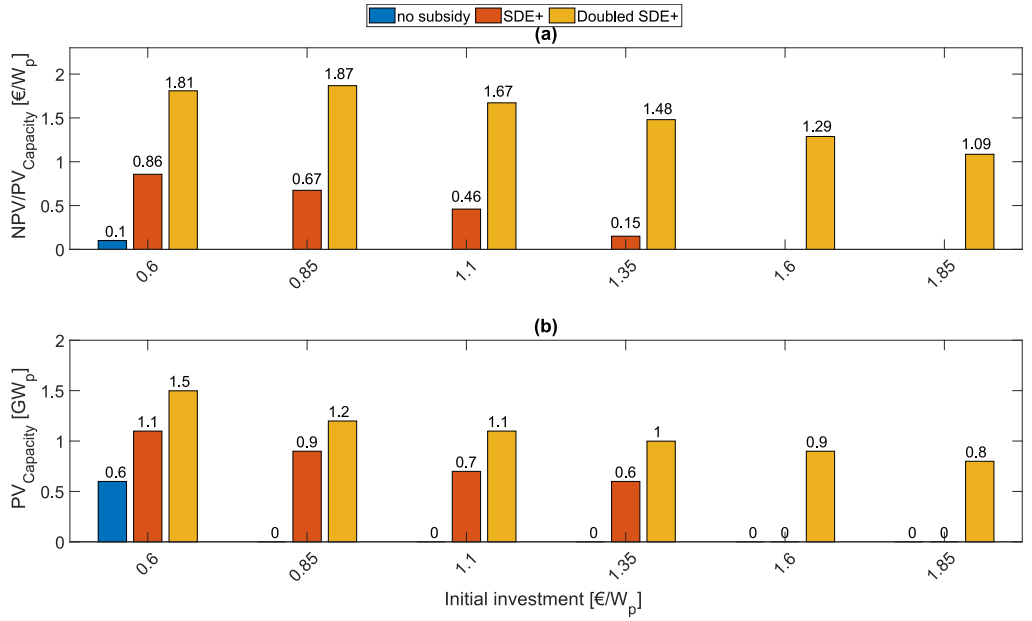

Fig. 8. (a) Ratio of *NPV* and PV capacity, (b) optimum PV capacity for the system based on initial investment [$€$/Wp].

$$E_{opt,PV} = \sum_n \left(\sum_h P_{PVF} Y_{PV}(h) \times (1 - d_{r,PV})^n \right) - \left[P_{cable} - \sum_n \left(\sum_h P_{WF} Y_W(h) \times (1 - d_{r,W})^n \right) \right] \quad (23)$$

Obviously, with higher cost per Wp, optimum PV capacity decreases, but more favourable subsidies lead to a higher optimized PV capacities. It is clearly shown that for solving this optimization problem many aspects should be considered which will be discussed more generally in the next subsection.

3.3.1. Generalisations

From the above we can generalize the optimization of combined wind and solar parks. Given site-specific meteorological conditions (wind, irradiation, temperature) one should calculate specific hourly energy generated $Y_W(h)$ and $Y_{PV}(h)$ in kWh/kWp, for both wind and solar capacity, P_{WF} and P_{PVF}, respectively. Optimization of the combined wind and solar park in combination with cable capacity P_{cable} can be

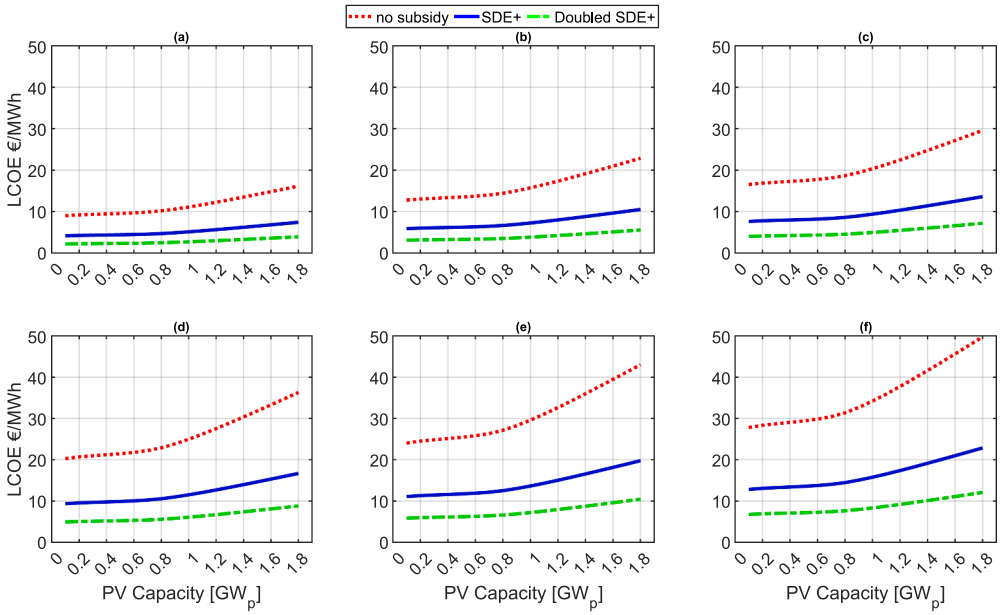

Fig. 9. Variation of *LCOE* with PV capacity for different scenarios considering the initial investment: (a) 0.6, (b) 0.85, (c) 1.1, (d) 1.35 , (e) 1.6, (f) 1.85 [€/Wp].

done by calculating the additional energy from the solar power system as:

where $d_{r,i},\ i \in [PV, W]$ is degradation factor for system *i*, and referring to Eq. (17) specific hours of power generation are based on the peak and off-peak classification we used above:

$$Y_i = Y_{i,p} + Y_{i,op},\ i \in [PV, W] \tag{24}$$

The optimization problem is generalized in Eq. (25). *NPV* should be calculated as mentioned in Eq. (20),

$$\max\{NPV\},\ \texttt{for}\ \{P_{WF}, P_{PVF}\}\ \textbf{subject to}\ \{P_{cable}\ \&\ E_{opt,PV}\} \tag{25}$$

Two important constraints for this problem are the cable capacity and $E_{opt,PV} > 0$. In this study, the optimum additional floating solar energy system is discussed considering both technical and economical aspects. First, generated solar energy regarding the generated wind energy and cable capacity is calculated. To solve the optimization problem further information is required namely, initial investment per Wp for the floating PV system. Calculating *NPV* clarifies the economic analysis of the system. For an acceptable project we need to solve the problem $NPV = 0$, the system is profitable if $NPV > 0$. The aforementioned case study showed that the relation between *NPV* and PV capacity is not linear, which means that increasing the solar capacity does not necessarily lead to higher revenues or lower LCOE for the project. Fig. 8 shows that this system without subsidy could be profitable only if:

$$f_{0,FPV} \leqslant f_{0,LB} \tag{26}$$

However, for the SDE + scenario this system could be profitable even if:

$$f_{0,FPV} \leqslant 2.67 \times f_{0,LB} \tag{27}$$

and with doubled SDE + the system is profitable for all considered values in this study.

Fig. 8 indicates the optimum PV capacity for each scenario, derived from Fig. 7. For this comparison the PV capacities between zero and 1.9 GWp are studied and a clear trend is observed. The ratio of *NPV* and PV capacity is decreasing with increasing initial investment. Also, the optimum PV capacity is decreasing with increasing initial investment. It is clear that a subsidy is essential for this project in case the initial investment for the floating PV system is higher than 140% of the land-based PV system. The associated *LCOE* values are shown in Fig. 9, and reflect the variation in *NPV* and PV capacity. Also, the higher the subsidy, the lower the *LCOE*. We note that these values compare well with recently published values (Rosa-Clot and Tina, 2020), but also show that subsidies are necessary to obtain $LCOE < 0.05$ €/kWh, which are current generating costs of fossil-fuel based electricity generating plants in the Netherlands.

4. Conclusion

The combination of an offshore solar PV system and a wind farm can be beneficial in technical and economical terms. At times with sub-optimal power generation by wind turbines the cable that transports electricity to the coast is not optimally used either. Adding solar capacity increases cable usage, which is known as cable pooling. We have calculated optimal wind and solar combined capacity given meteorological conditions in the North Sea, showing that curtailment of solar is quite limited.

The economical analysis showed that the profitability of integrating floating PV within offshore wind farms depends on two major factors: the marginal power delivered to the grid by floating PV and the costs of the solar system. Improving the marginal solar power delivered to the grid and decreasing the total costs for the offshore FPV system would result in larger total benefits. We have also shown that subsidy is needed at present to support offshore FPV deployment.

Finally, our case study is further generalized realizing that meteorological conditions, in particular the anti-correlation of the wind and solar resource is determining, next to cost, the optimum wind-solar combination.

Declaration of Competing Interest

The authors declare that they have no known competing financial interests or personal relationships that could have appeared to influence the work reported in this paper.

Acknowledgements

The authors gratefully acknowledge fruitful discussions with Brigitte Vlaswinkel (Oceans of Energy), Anne de Waal (UU), and Geert Harm Boerhave (RVO). This work is partly financially supported by the

Netherlands Enterprise Agency (RVO) within the framework of the Dutch Topsector Energy (project Comparative assessment of PV at Sea versus PV on Land, CSEALAND).

References

Arrambide, Iñaki, Zubia, Itziar, Madariaga, Ander, 2019. Critical review of offshore wind turbine energy production and site potential assessment. Electric Power Syst. Res. 167, 39–47.

Astariz, S., Iglesias, G., 2016. Output power smoothing and reduced downtime period by combined wind and wave energy farms. Energy 97, 69–81.

Beurskens, L.W.M., Lensink, S.M., 2017. Kosten wind op zee 2017. Technical report, Energy Research Centre of the Netherlands (ECN).

Brown, Tom W, Bischof-Niemz, Tobias, Blok, Kornelis, Breyer, Christian, Lund, Henrik, Mathiesen, Brian, V., 2018. Response to 'burden of proof: A comprehensive review of the feasibility of 100% renewable-electricity systems'. Renew. Sustain. Energy Rev. 92, 834–847.

Bulder, B.H., Bot, E.T.G., Wiggelinkhuizen, E.J., Nieuwenhout, F.D.J., 2014. Quick Scan Wind Farm Efficiences of the Borssele Location, Technical report. Energy Research Centre of the Netherlands (ECN).

Cazzaniga, R., Cicu, M., Rosa-Clot, M., Rosa-Clot, P., Tina, G.M., Ventura, C., 2018. Floating photovoltaic plants: Performance analysis and design solutions. Renew. Sustain. Energy Rev. 81, 1730–1741.

Dutch New Energy Research, 2020. Nationaal Solar Trendrapport. Technical report.

Copernicus Atmosphere Monitoring, Service. https://atmosphere.copernicus.eu.

Exasun, 2018. Black glassTM "power that lasts. data-sheet. https://exasun.com/wp-content/themes/exasun/images/2018/10/20182610-Black-Glass-Datasheet.pdf.

Farfan, Javier, Breyer, Christian, 2018. Combining floating solar photovoltaic power plants and hydropower reservoirs: a virtual battery of great global potential. Energy Procedia 155, 403–411.

Folkers, W., van Sark, W., de Keizer, C., van Hooff, W., van den Donker, M., 2017. Roadmap pv systems and applications. Study commissioned by the Netherlands Enterprise Agency (RVO) in collaboration with the TKI Urban. Energy.

Gielen, Dolf, Boshell, Francisco, Saygin, Deger, Bazilian, Morgan D., Wagner, Nicholas, Gorini, Ricardo, 2019. The role of renewable energy in the global energy transformation. Energy Strategy Rev. 24, 38–50.

Jäger-Waldau, Arnulf, 2019. PV status report 2019. Technical report, European Commission's science and knowledge service.

Jäger-Waldau, Arnulf, 2020. The untapped area potential for photovoltaic power in the European Enion. Clean Technol. 2 (4), 440–446.

Jensen, N.O., 1983. A note on wind generator interaction, Technical report, Risø National Laboratory, Risø-M No. 2411.

Jordan, Dirk C, Kurtz, Sarah R, 2012. Photovoltaic degradation risk. Technical report, National Renewable Energy Lab.(NREL), Golden, CO (United States).

Karpouzoglou, Thodoris, Vlaswinkel, Brigitte, van der Molen, Johan, 2020. Effects of large-scale floating (solar photovoltaic) platforms on hydrodynamics and primary production in a coastal sea from a water column model. Ocean Sci. 16 (1), 195–208.

Katic, I., Højstrup, J., Jensen, N.O., 1987. A simple model for cluster efficiency. Proceedings EWEC'86, pp. 407–410.

Ministry of Economic Affairs and Climate, 2020. Sde+ spring 2020, instructions on how to apply for a subsidy for the production of renewable energy. Technical report.

Nordmann, T., Clavadetscher, L., van Sark, W., Green, M, 2015. Analysis of long-term performance of PV systems. IEA-PVPS, Report IEA-PVPS T13-05:2014.

Orsted. Eerste turbine borssele 1&2 geïnstalleerd, https://orsted.nl/news-archive/2020/04/eerste-turbine-borssele-1-2-geinstalleerd.

Ram, Manish, Bogdanov, Dmitrii, Aghahosseini, Arman, Oyewo, Solomon, Gulagi, Ashish, Child, Michael, Fell, Hans-Josef, Breyer, Christian, 2017. Global energy system based on 100% renewable energy–power sector. Lappeenranta University of Technology and Energy Watch Group, Lappeenranta, Finland.

Randle-Boggis, R.J., White, Piran Crawfurd Limond, Cruz, Joana, Parker, Guy, Montag, Hannah, Scurlock, J.M.O., Armstrong, Alona, 2020. Realising co-benefits for natural capital and ecosystem services from solar parks: a co-developed, evidence-based approach. Renew. Sustain. Energy Rev. 125 (2020) 109775.

Reich, Nils H., Mueller, Bjoern, Armbruster, Alfons, Van Sark, Wilfried G.J.H.M, Kiefer, Klaus, Reise, Christian, 2012. Performance ratio revisited: is PR 90% realistic? Prog. Photovolt. Res. Appl. 20 (6), 717–726.

Rijksoverheid, 2019. Kamerbrief moties Dik-Faber over zonneladder als nationaal afwegingskader bij inpassing van zonne-energie. Technical report, Rijksoverheid.

Rosa-Clot, Marco, Tina, Giuseppe Marco, 2017. Submerged and Floating Photovoltaic Systems: Modelling. Academic Press, Design and Case Studies.

Rijksdienst voor Ondernemend Nederland, 2019. Appendices hollandse kust (zuid) wind farm sites iii and iv. Technical report, RVO.

Rosa-Clot, M., Tina, G.M., 2020. Chapter 10 - levelized cost of energy (LCOE) analysis. Academic Press, pp. 119–127.

Sahu, Alok, Yadav, Neha, Sudhakar, K., 2016. Floating photovoltaic power plant: A review. Renew. Sustain. Energy Rev. 66, 815–824.

Scognamiglio, Alessandra, Garde, François, 2016. Photovoltaics' architectural and landscape design options for net zero energy buildings, towards net zero energy communities: spatial features and outdoor thermal comfort related considerations. Prog. Photovolt.: Res. Appl. 24 (4), 477–495.

Siemens, Gamesa. https://www.siemensgamesa.com/products-and-services/offshore/wind-turbine-sg-8-0-167-dd.

Staffell, Iain, Green, Richard, 2014. How does wind farm performance decline with age? Renewable Energy 66, 775–786.

Tennet. https://www.tennet.eu/news/detail/borssele-alpha-offshore-grid-connection-ready-for-north-sea-wind-power/.

Van Sark, W.G.J.H.M., Bosselaar, L., Gerrissen, P., Esmeijer, K., Moriatis, P., Van den Donker, M., Emsbroek, G., 2014. Update of the Dutch PV specific yield for determination of PV contribution to renewable energy production: 25% more energy! 29th European Photovoltaic Solar Energy Conference and Exhibition, pp. 4095–4097.

van Zalk, John, Behrens, Paul, 2018. The spatial extent of renewable and non-renewable power generation: A review and meta-analysis of power densities and their application in the us. Energy Policy 123, 83–91.

Venkataraman, Sundar, Ziesler, Chris, Johnson, Peter, Van Kempen, Stephanie, 2018. Integrated wind, solar, and energy storage: Designing plants with a better generation profile and lower overall cost. IEEE Power Energ. Mag. 16 (3), 74–83.

Vermeer, L.J., Sørensen, J.N., Crespo, A., 2003. Wind turbine wake aerodynamics. Prog. Aerosp. Sci. 39 (6), 467–510.

Wijnant, I.L., van Ulft, B., van Stratum, B., Barkmeijer, J., Onvlee, J., de Valk, C., Knoop, S., Kok, S., Marseille, G.J., Klein Baltink, H., Stepek, A., 2019. The Dutch Offshore Wind Atlas (DOWA): Description of the Dataset, Report TR-380, Technical Report. Royal Netherlands Meteorological Institute (KNMI).

Zahra Golroodbari, S., van Sark, Wilfried, 2020. Simulation of performance differences between offshore and land-based photovoltaic systems. Prog. Photovolt. Res. Appl. 28, 873–886.